

Naval Research Laboratory

Washington, DC 20375-5000

AD-A253 353



2

NRL/MR/4440-92-6998

Molecular Dynamics of Shocks in Crystals with Defects

LEE PHILLIPS, ROBERT S. SINKOVITS, ELAINE S. ORAN, AND JAY P. BORIS

Laboratory for Computational Physics and Fluid Dynamics

July 15, 1992

DTIC
ELECTE
JUL 29 1992
S D

92-20352



Approved for public release; distribution unlimited.

92 7 28 005

REPORT DOCUMENTATION PAGE			Form Approved OMB No. 0704-0188	
Public reporting burden for this collection of information is estimated to average 1 hour per response, including the time for reviewing instructions, searching existing data sources, gathering and maintaining the data needed, and completing and reviewing the collection of information. Send comments regarding this burden estimate or any other aspect of this collection of information, including suggestions for reducing this burden, to Washington Headquarters Services, Directorate for Information Operations and Reports, 1215 Jefferson Davis Highway, Suite 1204, Arlington, VA 22202-4302, and to the Office of Management and Budget, Paperwork Reduction Project (0704-0188), Washington, DC 20503.				
1. AGENCY USE ONLY (Leave blank)	2. REPORT DATE July 15, 1992	3. REPORT TYPE AND DATES COVERED Interim		
4. TITLE AND SUBTITLE Molecular Dynamics of Shocks in Crystals with Defects		5. FUNDING NUMBERS NRL/MR/4440-92-6998		
6. AUTHOR(S) Lee Phillips, Robert S. Sinkovits, Elaine S. Oran, and Jay P. Boris				
7. PERFORMING ORGANIZATION NAME(S) AND ADDRESS(ES) Naval Research Laboratory Washington, DC 20375-5000		8. PERFORMING ORGANIZATION REPORT NUMBER PE - 61153N PR - RR011030K WU - 1950		
9. SPONSORING / MONITORING AGENCY NAME(S) AND ADDRESS(ES) Office of Naval Research 800 N. Quincy Street Arlington, VA 22217-5999		10. SPONSORING / MONITORING AGENCY REPORT NUMBER		
11. SUPPLEMENTARY NOTES				
12a. DISTRIBUTION / AVAILABILITY STATEMENT Approved for public release; distribution unlimited.		12b. DISTRIBUTION CODE		
13. ABSTRACT (Maximum 200 words) We examine, using computational molecular dynamics, shocks launched in two-dimensional crystals by a flying plate. The interaction of the shock with various lattice defects is observed, and is seen to create sites of rapidly growing, thermalized, hot fluid-like phases included within the crystal lattice. We hypothesize that these included fluid-like regions are the sites of the initial chemical reactions leading to detonation in energetic materials, and that crystallographic defects therefore control the sensitivity of single crystal high explosives to shock-initiation. The computations are carried out on the massively parallel Connection Machine using a parallelized version of the MLG algorithm.				
14. SUBJECT TERMS Detonation Defects Molecular dynamics			15. NUMBER OF PAGES 44	
			16. PRICE CODE	
17. SECURITY CLASSIFICATION OF REPORT UNCLASSIFIED	18. SECURITY CLASSIFICATION OF THIS PAGE UNCLASSIFIED	19. SECURITY CLASSIFICATION OF ABSTRACT UNCLASSIFIED	20. LIMITATION OF ABSTRACT UL	

CONTENTS

1. INTRODUCTION	1
2. METHOD	6
3. RESULTS	9
4. CONCLUSIONS	16
ACKNOWLEDGMENTS	17
REFERENCES	19

Accession For	
NTIS GRA&I	<input checked="" type="checkbox"/>
DTIC TAB	<input type="checkbox"/>
Unannounced	<input type="checkbox"/>
Justification	
By _____	
Distribution/	
Availability Codes	
Dist	Avail and/or Special
A-1	

DTIC QUALITY INSPECTED 2

Molecular Dynamics of Shocks in Crystals with Defects

1 INTRODUCTION

This paper investigates, on the molecular scale, the propagation of vibrational disturbances through various two-dimensional lattices, using the techniques of computational non-equilibrium molecular dynamics. These disturbances will be referred to as "shocks", as is common in the literature, because, although they have a finite width and a definite structure, they are thought to be the microscopic analogues of the travelling discontinuities that are defined as shocks in the macroscopic domain of continuum mechanics.

The motivation behind the work reported in this paper is the desire to understand some of the peculiar properties of the initiation and propagation of detonations in solid chemical explosives. A detonation, as the term is usually understood in these contexts, is a physico-chemical process with a characteristic structure.¹ This structure consists, in a solid, liquid, or gas, of a shock wave or some other localized, traveling disturbance, followed by an associated reaction front, which separates material that has participated in a chemical reaction from material that is not yet reacted. The association between these two traveling interfaces, mediated by the "induction zone" of (usually) compressed, stressed, unreacted material between them, is a complex interdependence whose nature has been the subject of many investigations, a few of which we shall discuss below. For now we should

Manuscript approved May 13, 1992.

merely point out that, on the one hand, the shock is the cause of the reaction front, for in its passage it creates the conditions which lead to a particular series of reactions, while, on the other hand, the exothermic reaction front maintains and accelerates the shock by supplying kinetic and thermal energy.

In the fluid phases, those properties governing the nature of the detonation process are the chemical composition of the material along with its intensive thermodynamic variables, and, sometimes, the details of the method used to initiate the detonation. In a solid, even when all of these quantities are held constant, there may still be significant variability in the responses of a series of samples. For example, in an experiment in which crystals are detonated by dropping a weight on them, the variability may take the form of a wide range of initial heights necessary for detonation in apparently identical samples. A possible source of this variable response might be some unknown and uncontrolled variation in the experimental conditions, presenting different samples with significantly different initial conditions, combined with an extreme sensitivity to initial conditions in the system. But it must be recognized that a sample of solid material, unlike a fluid, is characterized not only by its chemical composition and its thermodynamic state. The particular spatial arrangement of molecules constituting each sample makes them all unique. The fact that the shock, solitary compressional wave, or other disturbance taking part in the structure of the detonation process is a mechanical mode of vibration supported by the molecular lattice, whose nature is completely dependent on the detailed structure of that lattice, implies that the spatial arrangement of molecules must influence the detonation process. This much is uncontroversial. What may be more surprising is the suggestion² investigated here, that certain minute changes in the molecular arrangement, involving the locations of just a few molecules, may have a large, even determining, effect on a macroscopic detonation. This suggestion gains plausibility if one considers that the actual thickness of the shock front may be only a few lattice planes.³ Therefore the transfer of kinetic energy from a molecule to its neighbors in the direction of propagation involves the participation of only a few molecules (along the wavevector direction) in a particular vibrational mode

at any one time.

One traditional theoretical approach to understanding detonations, and the initiation of a detonation by a shock wave, involves a description in terms of thermodynamic variables that are related by an equation of state for the material.¹ The passage of the shock heats the material through adiabatic compression; if the compression is great enough, then the local temperature will rise to a threshold required to initiate the chemical reactions, and a reaction front will form behind the shock. In practice, the equations of state for energetic materials are quite complex, and feature many empirical parameters, whose adjustment allows the theory to agree quite well with preexisting experimental data.

However, for understanding the detailed microscopic nature of detonations in a solid, the traditional theories may not be appropriate. At the scale of intermolecular distances, the usefulness of thermodynamic variables is problematic, and at timescales shorter than nanoseconds, relations built upon the assumption of thermodynamic equilibrium require special scrutiny (the rapid approach to thermal equilibrium under some circumstances is discussed further in section 3.) We should point out that a description based on classical mechanics, such as that employed here, must also be insufficient, but can form the basis for more accurate quantum or semi-classical descriptions.

In this paper we examine the point of view, championed by Walker,⁴⁻⁷ that a shock in a solid initiates detonation through the mechanical generation of scission forces on the molecules comprising the solid, breaking chemical bonds, creating a distribution of free radicals, and supplying the kinetic energy required to initiate reaction. In the light of this picture of the detonation process, we investigate the interaction of the shock front with the lattice structure, using numerical molecular dynamics. We are particularly interested in the effects of certain types of lattice defects on the shock initiation mechanism. We include no chemistry in our model; the "molecules" are point particles interacting through Lennard-Jones potentials. Hence our current connection to the detonation problem is the exploration of how the conditions leading to bond scission and subsequent recombination are established. The following stage, of reaction and shock acceleration, will be treated in

a subsequent paper, which will report on simulations employing a chemistry model.

There have been reported a number of interesting molecular dynamics calculations that bear, in one way or another, on the problem of the shock initiation of detonations in solids. Karo *et al.*⁸ simulated a small lattice of approximately one hundred molecules arranged in a two-dimensional square-symmetric lattice, interacting through either "endothermic" Morse potentials or "exothermic" polynomial potentials. A shock was launched by simulating a flying plate consisting of a smaller lattice of identical construction to the main lattice. (This is quite similar to our method of shock launching in this paper.) The main conclusions were that the shock was quite narrow on the atomic scale, that the temperature of the lattice was unimportant, and that the free surface at the end of the finite lattice was a crucial feature, as the shock's interaction with this surface resulted in a spalling off of a large chunk of the crystal. The behavior subsequent to the spalling depended on which potential was in use. With the endothermic potential, there was little interesting activity after the separation of the chunk, but with the exothermic potential, a violent reorganization of the lattice occurred.

While there is little reason to question the reliability of the general character of the results reported in these seminal papers, especially the importance of free surfaces, there are several numerical issues that should be discussed. Unfortunately, issues of convergence and accuracy are not treated in these references: conserved quantities are not mentioned, nor are the methods of integration. Instead of physically faithful additive potentials, the authors employ two different first- and second-neighbor potentials chosen to make the initial lattice stable. In addition, as the lattice undergoes its natural distortion and molecules acquire different sets of close neighbors, they are not allowed to interact with these new neighbors. Instead, the original table of bonds is used throughout the calculation. As the authors point out, this leads at times to molecules passing through each other without interaction. (Indeed, this is a statistical possibility, albeit of low likelihood,⁹ with the method we employ, as discussed below.) One of our goals in the work reported here is to discover which of these results survive the application of more modern numerical

methods applied to somewhat more realistic simulations.

Later,¹⁰ using the same numerical method, these authors studied a shock in a lattice interrupted by a large gap consisting of a region with no molecules. As before, they observed spall from the free surface, with this time the spalled molecules reaching the second free surface beyond the gap and launching a second shock. This was an attempt to simulate efficiently the behavior of a true void in a crystal, which would be surrounded by the lattice on all sides and make up a small fraction of the lattice. As we discuss in the section 3, our simulations of small true voids included in a large lattice lead to somewhat different conclusions from simulations employing a gap.

In more recent, related work, these authors and others¹¹⁻¹³ embed a computational surrogate for a polyatomic molecule into a simple host lattice, and show how the passage of the shock pumps energy directly into some of the vibrational modes of the molecule. This pumping could lead directly to bond scission in a real material, in a region that is definitely not ergodic, and where no thermodynamic temperature can be defined.

Also relevant is the work of Tsai and Trevino¹⁴ on a diatomic perfect crystal in the form of a long filament with a small cross-section. Exothermic bond breaking was simulated through the use of bound and free compound Morse potentials, and the shock was formed by heating the first six crystal planes. The initial temperature of their lattice was set at just below the threshold of spontaneous dissociation; the heating caused dissociation directly, the reaction spread by thermal conduction and drove a shock wave into the filament. They kept track of the stresses and examined the partition of kinetic energy in the induction zone, concluding that thermal equilibrium was not reached before dissociation took place. There is no discussion of numerical accuracy or the treatment of distant neighbors, although presumably the expediency of imposing a cutoff distance on the potentials, as adopted in a previous paper,¹⁵ was used here as well.

Several authors have demonstrated that the typical quasi-steady detonation structure, described above, is predicted by molecular dynamics models, with the exothermic reactive process modeled either by classical potentials acting between diatomic bonds^{16,9} or by

a more elaborate procedure that captures some of the features of the quantum chemical processes involved.¹⁷⁻²¹ All of these calculations involve perfect crystals, and although some of them examine the effects of lattice geometry, shock direction relative to lattice symmetry, etc., none of them deal with the action of crystallographic defects. A recent exception is the work of Maffre and Peyrard,²² which deals with the ability of a developed detonation structure to traverse grain boundaries, voids, and other localized defects. However they do not deal with the effect of defects in the transition from a pure shock to a detonation. Another exception is the recent work of Tsai,²³ which will be discussed below.

2 METHOD

Our model system consists of an array of point particles, each with a specified initial position and velocity vector, arranged in a two-dimensional space with either periodic or free boundary conditions in both directions. The algorithms were chosen for their convenience and efficiency on the computer used, the Connection Machine CM-200, which consists of a large number (4096, 8192, or 16384, depending on configuration) of processors, each with its own set of locally stored data, updated in parallel according to instructions from a controlling, "front-end" computer. Efficiency consists here largely of maximizing the proportion of code that executes in parallel, which entails minimizing the manipulation of front-end (global) data and maintaining careful control over the pattern of communication among processors.

Forces between particles were represented by Lennard-Jones potentials. The solution of the complete N-body problem was not attempted; rather, the short-range nature of the Lennard-Jones potential was exploited to limit the distance over which interactions had to be computed. The particle data was distributed onto a data structure known as the Monotonic Lagrangian Grid (MLG).²⁴ This is an object tracking and sorting technique where each particle is associated with a pair of integer indices i and j , and the assignment is ordered such that the coordinate x increases monotonically with i , and y increases

monotonically with j . Monotonicity was enforced after each update in particle positions by a parallel version of the swapping routine described in reference 24. The advantage of this method is that, at each timestep, a particle's neighbors can be identified quickly by cycling over a predetermined region of $i - j$ space, rather than by searching through coordinate space with an expensive comparison of particle separations.

Each physical processor on the Connection Machine can be divided, in software, into as many virtual processors as memory will allow. When we refer to a "processor" from here on, this should be taken to mean "virtual processor". One particle was associated with each processor, which stored the particle's position and velocity coordinates, as well as any other information unique to the particle. We also stored a near neighbors template²⁴ in each processor; this is an array that stores the position information for each particle's neighbors in grid-index space. Once the template is filled, the total force vector acting on each particle and the update in position is computed for all particles entirely in parallel, with no additional interprocessor communication needed for the rest of the timestep. After each regeneration of the MLG by the swapping routine, the template is rebuilt; thus each processor-particle always has a locally stored, updated list of the coordinates of its near neighbors. The use of the MLG is one of several available efficient schemes for replacing a time consuming search for the spatially proximate neighbors of each particle at every timestep. However, as alluded to in the Introduction, its use can lead occasionally (but infrequently) to the problem of missed near neighbors,²⁴ particles that are spatially close but not included in the neighbor template. When these near-misses are detected by a failure of energy conservation or repeatability, we redo the calculation with a larger template. Thus the template size is treated like the computational timestep, both of which are adjusted to keep the calculations stable and accurate.

The procedure for filling up the template at each timestep is an important determinant of the overall efficiency of the algorithm. Interprocessor communication between neighboring processors happens to be far more efficient than between more distant processors, so we fill the template using a sequence of coordinated data moves between neighboring pro-

cessors only. The total number of these parallel move operations is equal to one less than the total number of elements in the template array; therefore the total time required to fill the template depends on its size, not on the number of particles (assuming that the ratio of virtual processors to physical processors remains constant). Part of the communication sequence is diagrammed schematically in figure 1.

As the studies described in this paper were being carried out, the computer hardware and system software being used was evolving. Fortunately, only one of these changes needs to be discussed here: initially, the Connection Machines that were used for these calculations were equipped with floating-point accelerators that operated on 32-bit numbers only; more recently, we were provided with 64-bit accelerators.

For reasonable efficiency, it is necessary to restrict the precision of floating point numbers to the word size of the accelerator. Therefore, some of the results reported here were performed with 32 bit arithmetic, some with 64 bit, and some of the 32 bit calculations were redone with 64 bits ("double precision") when that became available. The small differences we observed in particle data between the two precisions was not significant enough to affect our conclusions. The chief advantage to the greater precision will be for future calculations, which we will be able to carry out for longer times before the accumulated errors become unacceptable.

We found that single precision arithmetic limited the accuracy with which energy can be conserved, and made the extra accuracy of higher-order time integration methods superfluous, and their use needlessly time consuming. Therefore some of the results reported here were calculated with the simple explicit Euler method. We were able to achieve stability with this method using a reasonable timestep. The consequence of the limitation of precision is that energy is conserved only to approximately one percent in the 32 bit calculations. With double precision arithmetic, it became advantageous to use a higher-order integrator. We have used both the leapfrog method (described in several places, for instance²⁵) and the third order Verlet formula²⁶ combined with a velocity corrector described by Beeman.²⁷ The advantage of this method (described at the bottom of page 138

of reference 27) is that the velocities do not have to be permanently stored, and need only be calculated when they are required for a data dump or a check of the kinetic energy. Our algorithm with these integrators can conserve energy to one part in 10^4 , in actual calculations.

We have performed calculations with three different system sizes, "small" grids of 2^{12} or 2^{13} molecules distributed among an equal number of physical processors, and a "large" grid of 2^{15} molecules distributed among 2^{14} physical processors, which is the largest processor set available to us. (Our original machine, with two banks of 2^{12} processors, was replaced partway through this project with one of two banks of 2^{13} processors.) In both cases each molecule was assigned its own virtual processor. All else being equal, the large grid should take approximately twice as long to simulate as the small grids, because it is the ratio of virtual to physical processors that is significant. On the small grids, with five neighbors in the template in each direction, the calculation took 0.67 seconds per timestep. On the large grid, a five-neighbor calculation took 1.0 seconds per timestep and a seven-neighbor calculation took 2.0 seconds per timestep. We have verified several of our runs with equivalent calculations on NRL's Cray X-MP, using a well-vectorized code. With 4096 molecules, a five-neighbor template takes 2-2.4 seconds per timestep; with larger system sizes, the disparity between the two architectures can be expected to grow dramatically.²⁸

3 RESULTS

It is difficult to compare directly the various molecular dynamics simulations that can be found in the literature, due to the varying sets of units employed by different authors, along with differences in potential parameters, lattice spacing, initial conditions, etc., each of which can have a nonobvious effect on the evolution of the system. Although the large number of parameters characterizing a molecular system makes a simple resort to dimensionless numbers impossible, it may be useful to introduce one such number, which can be used to organize the results concerning the type of molecular dynamics configuration

used in this paper.

We have an array of molecules with forces between them derived from a Lennard-Jones potential,

$$\phi = 4\epsilon \left[(\sigma/r)^{12} - (\sigma/r)^6 \right],$$

so the force, F , is given by

$$F = -\frac{d\phi}{dr} = 4\epsilon \left[-12 \frac{\sigma^{12}}{r^{13}} + 6 \frac{\sigma^6}{r^7} \right] = m \frac{d^2 r}{dt^2},$$

by Newton's equation of motion. In the above two equations r is the distance from the molecule, m is the molecular mass, t is time, and σ and ϵ are the two parameters characterizing the potential. In order to make the equation of motion dimensionless, we must introduce scales appropriate to a system excited by a flying plate:

$$d = \text{interparticle spacing} \quad V_p = \text{plate velocity} \quad \tau = d/V_p$$

$$\mu = \text{particle mass} \quad \Sigma = \mu d^2 / \tau^2 = \text{energy unit.}$$

After making the substitutions

$$r \rightarrow r'd \quad \epsilon \rightarrow \epsilon'\Sigma \quad t \rightarrow t'\tau \quad m \rightarrow m'\mu \quad \sigma \rightarrow \sigma'd$$

and removing the primes from the now dimensionless variables, the equation of motion becomes

$$\mathcal{L}^{-1} 4 \left[-12 \sigma^{12} / r^{13} + 6 \sigma^6 / r^7 \right] = m \frac{d^2 r}{dt^2},$$

where

$$\mathcal{L} \equiv \frac{V_p^2 \mu}{\epsilon}$$

emerges as a new dimensionless number, apparently relating the kinetic energy of the impacting molecules to the binding energy of the intermolecular potential.

In all of the calculations presented here, $\epsilon = 0.0223$, $\sigma = 0.891$, the plate velocity = 2.0, the intermolecular separation at equilibrium = 1.0, and the particle mass = 4.0, giving

$\mathcal{L} = 727.3$. It may help put things into context for some readers if we scale our variables to the values appropriate to solid argon, a substance commonly discussed. In this case the plate velocity scales to 4258 meters/second, one time unit is 0.88×10^{-13} seconds, and one distance unit is 3.8 Å. From here on we shall use the dimensionless units.

Figure 2 shows a sequence of molecular configurations as a plate-launched shock encounters a pair of voids, producing a great deal of disorder. The same initial conditions in a system without the voids lead to the shock traversing the crystal intact and leaving it undisturbed. We see here that the voids disturb the coherency of the shock, transforming its organized, x -directed (horizontal) motions into a thermalized, two-dimensional ($x-y$) motion; beyond the defects, the shock continues as several disconnected pieces. The progress of the shock can perhaps be more clearly visualized in figure 3, showing profiles of the horizontal velocity along different lines through the crystal. That these disordered regions are actually "thermalized" can be seen by looking at the speed distribution of the molecules in the crystal. Figure 4 is a series of speed histograms corresponding to the calculation illustrated in figure 2; superimposed on each histogram plot is the two-dimensional Maxwell-Boltzman distribution with a temperature derived from the average kinetic energy of all the particles. At early times we can see the speed distribution dominated by two values, the near zero speed of the particles locked into the near zero temperature lattice configuration, and the highest speed, equal to the plate velocity. As time advances we can see the velocity distribution filling in, but remaining non-Maxwellian. In the last frame of the figure we have plotted the distribution of a subset of the system at $t = 15$ (the configuration at this time is shown in Figure 15), the subset consisting of the particles in the chaotic region delimited by $x = 15$ and $x = 42$. The superimposed Maxwell-Boltzman curve corresponds to the kinetic temperature of the subset of particles under consideration; clearly this region of particles has rapidly attained a thermal equilibrium, indicating that the collisionality in the chaotic region is high.

A similar calculation can be seen in figure 5, with the square lattice replaced by an hexagonal lattice. In this case, also, the small void has been replaced by a single va-

cancy. We can see here that even in a lattice geometry with a higher binding energy, and with, unlike the square lattice, nonlinear stability against moderate temperatures, a small imperfection creates a large disruption.

The creation of disordered hot spots from shock-void interaction has also been seen in recent simulations by Tsai.²³ These disordered regions also have the property of being at a slightly higher density than the equilibrium lattice, as can be seen in the density plot of Figure 6.

The interaction of a shock front with a mass defect in square and hexagonal lattices can be seen in figures 7 and 8, both showing the effect of the inclusion of a molecule with a %50 mass excess. The effects are similar to but weaker than those caused by voids.

We have performed a series of experiments on systems identical to the ones shown in the figures, but at various temperatures and intermolecular potential well depths. At very small temperatures the perfect square lattice becomes unstable when struck by the plate, and begins to dissociate. This is true even if the potential well depth is increased by a factor of 45. The hexagonal lattice, however, is stable to impact by the flying plate over a wide range of temperatures, although at higher temperatures the shock front is less sharply defined. The effects of the various types of hexagonal lattice defects, and their relative importance, is not affected by temperature, but is strongly dependent on the intermolecular potential well depth. For a given shock strength and defect type, it appears that it is possible to increase the well depth to a point at which the lattice remains stable.

It is useful to quantify the concept of the strength of the effect of different types of lattice defects, or their efficacy in disrupting the crystal when interacting with a shock. For this purpose we have defined two "disruption factors", to be used with the two lattice symmetries. The disruption factors should be defined in such a way that the elastic deformation of the lattice due to the shock itself does not make a contribution. Therefore the disruption factors will be zero for the case of a shock traversing a defect-free crystal that remains intact.

We can define disruption factors that satisfy these criteria as follows. For the square

lattice the angular positions of the four nearest neighbors are found. The disruption factor, χ , for each particle is defined as

$$\chi = \sum_{i=1}^4 |\sin \theta_i \cos \theta_i|,$$

where the summation is over near neighbors. For a compression or rarefaction of the lattice due to the propagation of a shock along one of the principal crystal axes, the angular positions of the near neighbors should remain $0, \pm\pi/2$, and π resulting in a $\chi = 0$.

The hexagonal lattice disruption factor must be defined in a slightly different manner. The angular positions of the six near neighbors of each particle change as the shock propagates through the lattice. In this case the angular positions of the six near neighbors are first found. The neighbors in the lower half-plane are reflected into the upper half-plane. The near neighbors are then sorted into order of increasing angle. The disruption factor for the hexagonal lattice is defined as

$$\chi = \sin \theta_1 + \sin(\theta_3 - \theta_2) + \sin(\theta_5 - \theta_4) + \sin \theta_6.$$

In the case of a shock passing through a hexagonal lattice causing only a compression or rarefaction along the shock direction, θ_1 and θ_6 should remain 0 and π , respectively. The angles θ_3 and θ_2 should be equal and θ_5 and θ_4 should be equal. As in the square lattice, a zero disruption is calculated.

The total disruption of the lattice is calculated by summing the per particle disruption factor over all particles. The values of the total disruption correlate well with the apparent disruption found by visual inspection of the particle positions.

Figures 9 and 10 display χ as a function of time for an assortment of crystal defects, for the square and hexagonal lattices respectively. The greater importance of voids over mass defects is obvious, as is the unstable growth of the disordered region after the passage of the shock. Figure 9 also shows that the fastest growing disruption factor is found for an interstitial inclusion in a square lattice. The spatial configuration for such a system is

shown in figure 11. The closer packed hexagonal lattice does not provide an equilibrium position for an interstitial inclusion.

Another useful diagnostic summary of the state of the system is a histogram distribution of the near-neighbor angular positions, such as that shown in figure 12. This figure shows the evolution of the angular distribution for the case of a vacancy in a square lattice. The additional peaks which develop in the histogram distributions indicate that the lattice is beginning to locally undergo a transition from a square to a hexagonal state. For a hexagonal lattice formed by the displacement of every other column of atoms perpendicular to the shock direction together with a compression along the shock direction, the near neighbor angular positions should be $\pm\pi/6$, $\pm\pi/2$ and $\pm5\pi/6$. The peaks are not found exactly at these angles since the lattice has a square structure a short distance from the region of disturbance, resulting in a distorted hexagonal state.

Figure 13 shows a calculation similar to that shown in figure 2, but in a system of 32K molecules, with a distribution of voids whose positions, shapes, and sizes (ranging from single-site vacancies to voids of nine molecules) are determined by a random number generator. This is a first attempt at simulating a system approximating a part of a real crystal, with its natural distribution of defects. The basic process shown in figure 2 is repeated here: each void, including even the single-site vacancies, becomes the seed of a rapidly growing region of thermalized disorder, which blocks the progress of the shock. The shock becomes more tenuous as its organized x -momentum is equilibrated, and, in the absence of energy available from chemical reactions, eventually dies out.

It is of some relevance to the mechanical bond-scission view of detonation initiation⁴ to determine the character of the forces acting upon individual molecules. While the effect of intermolecular potentials on the breaking of bonds is complicated and difficult to treat faithfully with a classical description, we believe we can make some relevant observations. The quantities of interest are the components of the stress tensor at each molecule; however, since our "molecules" are point particles, with no preferred directions for bond breaking, a dilatory force along a certain axis combined with a compressional force along a different

axis can not be interpreted as an influence that would necessarily lead to the breaking of a bond. Our compromise is to look at the divergence of the force vector, $\nabla \cdot F$, a quantity that when positive indicates a net extensional force acting on the molecule. Figure 14 is a particle position plot corresponding to a frame of figure 2, but indicating which molecules are experiencing a positive force divergence and which are experiencing a negative $\nabla \cdot F$. We see from this figure that the molecules participating in the advance of the shock front are under a large compressional force, while some of the molecules in the disordered regions behind the shock have $\nabla \cdot F > 0$, and so are being "pulled apart" by their neighbors. However, the magnitude of $\nabla \cdot F$ for these molecules is much smaller than that for the compressed molecules in the shock front.

The spherically symmetric potential leads to two possible periodic equilibrium lattice symmetries: square and hexagonal. As can be seen in Figure 15, the agitation created by the void collapse has provided a section of the lattice the opportunity to relax to the other periodic state available to it: we see here and in various other runs the emergence of a localized hexagonal region. We use the term "relax" above because the hexagonal state is actually of slightly smaller potential energy. Accompanying this relaxation, therefore, must be the generation of some extra kinetic energy. A somewhat similar shock-induced phase transition was shown in reference 10 where a potential with two minima acted between molecules.

The assertion has been made¹⁰ that in order to understand the shock-void interaction it is not necessary to place the void interior to the crystal, but, in the interests of computational efficiency (which in this context means reducing the number of molecules that need to be tracked) it is sufficient to examine the interaction of the shock with a gap in the lattice. In figure 16 we show the results of a calculation in every way identical with that shown in figure 2, except that the two voids in figure 2 have been replaced with a gap extending across the entire crystal; the gap begins at the same x position as the leading edges of the voids, and has the same width. We can see from Figure 16 that the shock succeeds in traversing the gap while maintaining its coherency, and proceeds down the lattice,

leaving it undisturbed. Thus we see an essential physical difference between a gap and an included void: the presence of neighbor molecules transverse to the direction of progress of the shock causes energy to be removed from the shock and distributed among greater degrees of freedom, leading to a thermalized region. A related observation has recently been made by Maffre and Peyrard,²² who demonstrated the ability of a shock-reaction front structure to traverse a void in a lattice.

In addition to various systems of voids, we have simulated the encounter of a shock with a type of extended defect sometimes called a slip line; the evolution of the system is shown in figure 17, which contains a sequence of plots of the particle positions. The slip line can be seen at $x = 24.5$; there are also small voids at the top and bottom boundaries extending from the slip line, created by the periodic boundary conditions. Once again the voids are seeds of a single growing chaotic region (joined at the periodic boundary), while it is clear, by inspecting the central portion of the plots, that the shock traverses the slip line completely intact.

4 CONCLUSIONS

When a shock, sufficiently weak that it is able to traverse a *perfect* crystal without permanently disturbing the configuration of its lattice, encounters a void in the lattice, the void becomes the site of a rapidly growing thermalized, hot, fluid-like phase characterized by a high density and a high degree of collisionality. These characteristics should be conducive to the onset of chemical reactions, and, we suspect, it is in these regions that the reactions leading to the development of a shock-detonation structure begin. It seems probable, therefore, that the void distribution in the lattice is an important factor controlling the sensitivity to shock-initiation and the character of the subsequent detonation front development. A perfect crystal should be relatively insensitive. It is possible that in three dimensions, other types of defects will be seen to be equally important, but that will be treated in a subsequent paper.

As discussed above, in order to concentrate on the narrowly defined problem of shocks and defects in molecular crystals, with as few complications as possible, we have deferred including a model of the chemical bond and simulated the behavior of moderately large systems of indivisible molecules with spherically symmetrical potentials. This approach has the advantage that our results are independent of the details of any particular model of detonation chemistry or intramolecular behavior, several of which are referenced in the Introduction.

Although we have been able to resolve several issues concerning the importance of defects, there are some remaining ambiguities that will not be resolved until we include polyatomic molecules in the simulations. These have their counterpart in the uncertainties plaguing our knowledge of the bond scission process in a shocked crystal lattice. If the polyatomic bonds are broken in the shocked region, due to direct energy transfer from the shock to vibrational modes of the molecules, then the scission forces discussed above have little relevance, because they occur in the disordered regions behind the shock. In this case the importance of the defects is in the thermalization and mixing, which will provide enhanced opportunities for the free radicals, created in the shocked region, to recombine. Of particular relevance here is the observation that thermal equilibrium is established in the disordered region close behind the shock, on a very fast timescale, implying that equilibrium equations of state may be relevant after all to the detonation process. If the chemical bonds are not broken directly by the passing shock, then the scission forces may be responsible for bond stretching and breaking in the disordered region, where conditions prevail that will enhance the subsequent reactivity. The truth is that neither computational nor theoretical work to date is sufficient to resolve these uncertainties. We hope that these questions can be addressed in the next generation of simulations, involving both defects and chemical reactions in polyatomic crystal lattices large enough to capture their interaction.

ACKNOWLEDGMENTS

This work has benefited materially through discussions with Sam Lambrakos, Sam Tre-

PHILLIPS *et al.*: MOLECULAR DYNAMICS OF SHOCKS....

vino, and Donald Tsai. It was supported by the Naval Research Laboratory and by the Office of Naval Research.

References

- [1] W. Fickett and W. C. Davis. *Detonation*. U. of Cal. Press, Berkeley, 1979.
- [2] W. Sandusky et al. Deformation and shock loading studies on single crystals of ammonium perchlorate relating to hot spots. In *Proc. of the Ninth Symposium (International) on Detonation*, page 975, 1989.
- [3] A. N. Dremin and V. Yu. Klimenko. The effect of the shock-wave front on the origin of reaction. *Prog. Astro. Aero.*, 75:253-268, 1981.
- [4] F. E. Walker. The initiation and detonation of explosives: an alternative concept. LLNL Report UCRL-53860, Lawrence Livermore National Laboratory, 1988.
- [5] F. E. Walker and R. J. Wasley. *Propellants and Explosives*, 1:73, 1976.
- [6] F. E. Walker. *Propellants, Explosives, and Pyrotechnics*, 7:2, 1982.
- [7] F. E. Walker. Physical kinetics. *J. Appl. Phys.*, 63:5548, 1988.
- [8] A. M. Karo, J. R. Hardy, and F. E. Walker. Theoretical studies of shock-initiated detonations. *Acta Astronautica*, 5:1041, 1978.
- [9] S. G. Lambrakos, E. S. Oran, J. P. Boris, and R. H. Guirguis. Molecular dynamics simulation of shock-induced detonations in energetic solids. In *Proc. of Conf. on Shock Waves in Condensed Matter*, page 499, 1987.
- [10] J. R. Hardy, A.M. Karo, and F. E. Walker. Molecular dynamics of shock and detonation phenomena in condensed matter. In *Proc. of the 7th ICOGER*, page 209, 1979.

- [11] A. M. Karo, F. E. Walker, T. M. DeBoni, and J. R. Hardy. The simulation of shock-induced energy flux in molecular solids. In *Proc. of the 9th ICODERS*, page 405, 1983.
- [12] A. M. Karo and J. R. Hardy. Molecular dynamics simulations of energy transfer in shocked molecular systems. *Int. J. of Quantum Chem.: Quantum Chem. Symposium*, 20:763, 1986.
- [13] A. M. Karo J. R. Hardy and M. H. Mehlman. Microscopic simulations of shock propagation in condensed media: comparison between real time and frequency domains. In D. Bershader and R. Hanson, editors, *Proc. 15th Int. Symposium on Shock Waves and Tubes*, page 885. Stanford, 1986.
- [14] D. H. Tsai and S. F. Trevino. Simulation of the initiation of detonation in an energetic molecular crystal. *J. Chem. Physics*, 81:5636, 1984.
- [15] D. H. Tsai and S. F. Trevino. Molecular dynamical studies of the dissociation of a diatomic molecular crystal. i. energy exchange in rapid exothermic reactions. *J. Chem. Physics*, 79:1684, 1983.
- [16] M. Peyrard, S. Odier, E. Oran, J. Boris, and J. Schnur. Microscopic model for propagation of shock-induced detonations in energetic solids. *Phys. Rev. B*, 33:2350, 1986.
- [17] Donald W. Brenner and C. T. White. Chemical model for intrinsic detonation velocities. In press, 1991.
- [18] Donald W. Brenner, Mark L. Elert, and C. T. White. Incorporation of reactive dynamics in simulations of chemically sustained shock waves. In *Proc. of Topical Conf. on Shock Compression of Condensed Matter*, page 263, 1989.

- [19] Mark L. Elert, David M. Deaven, Donald W. Brenner, and C. T. White. One-dimensional molecular dynamics simulation of the detonation of nitric oxide. *Phys. Rev. B*, 39:1453, 1989.
- [20] S. G. Lambrakos, M. Peyrard, E. S. Oran, and J. P. Boris. Molecular-dynamics simulation of shock-induced detonations in solids. *Phys. Rev. B*, 39:993, 1989.
- [21] S. G. Lambrakos and M. Peyrard. Modeling complex intramolecular processes using constrained molecular dynamics. *J. Chem. Physics*, 93:4329-4338, 1990.
- [22] P. Maffre and M. Peyrard. Simulations of impact-induced detonations in two-dimensional energetic solids: ideal and heterogeneous diatomic molecular crystals. In preparation, 1991.
- [23] D. H. Tsai, 1991. Private communication.
- [24] S. G. Lambrakos and J. P. Boris. Geometric properties of the monotonic lagrangian grid algorithm for near neighbor calculations. *Journal of Computational Physics*, 73:183, 1987.
- [25] M. K. Memon, R. W. Hockney, and S. K. Mitra. Molecular dynamics with constraints. *Journal of Computational Physics*, 43:345-356, 1981.
- [26] L. Verlet. *Physical Review*, 159:98, 1967.
- [27] D. Beeman. *Journal of Computational Physics*, 20:130, 1976.
- [28] B. G. J. P. T. Murray, Paul A. Bash, and Martin Karplus. Molecular dynamics on the connection machine system. Technical Report CB88-3, Thinking Machines Corporation, 1988.

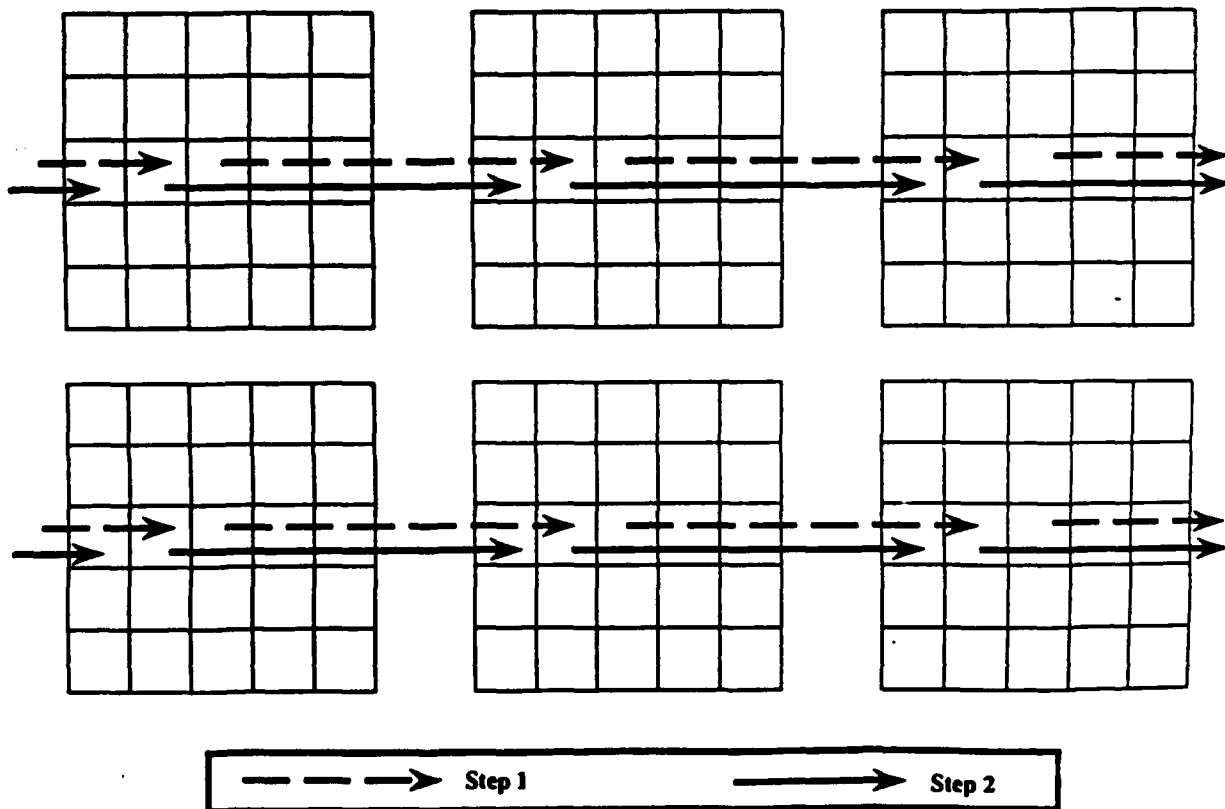


Figure 1: The two initial steps in a sequence of parallel move operations; the simplified case of a two-neighbor template is shown as an illustrative example, and the templates for six of the particles are included. Each processor's template is seeded at its center with its own particle's data; the arrows represent the copying of particle data from a template entry to the appropriate template entry in a neighboring processor.

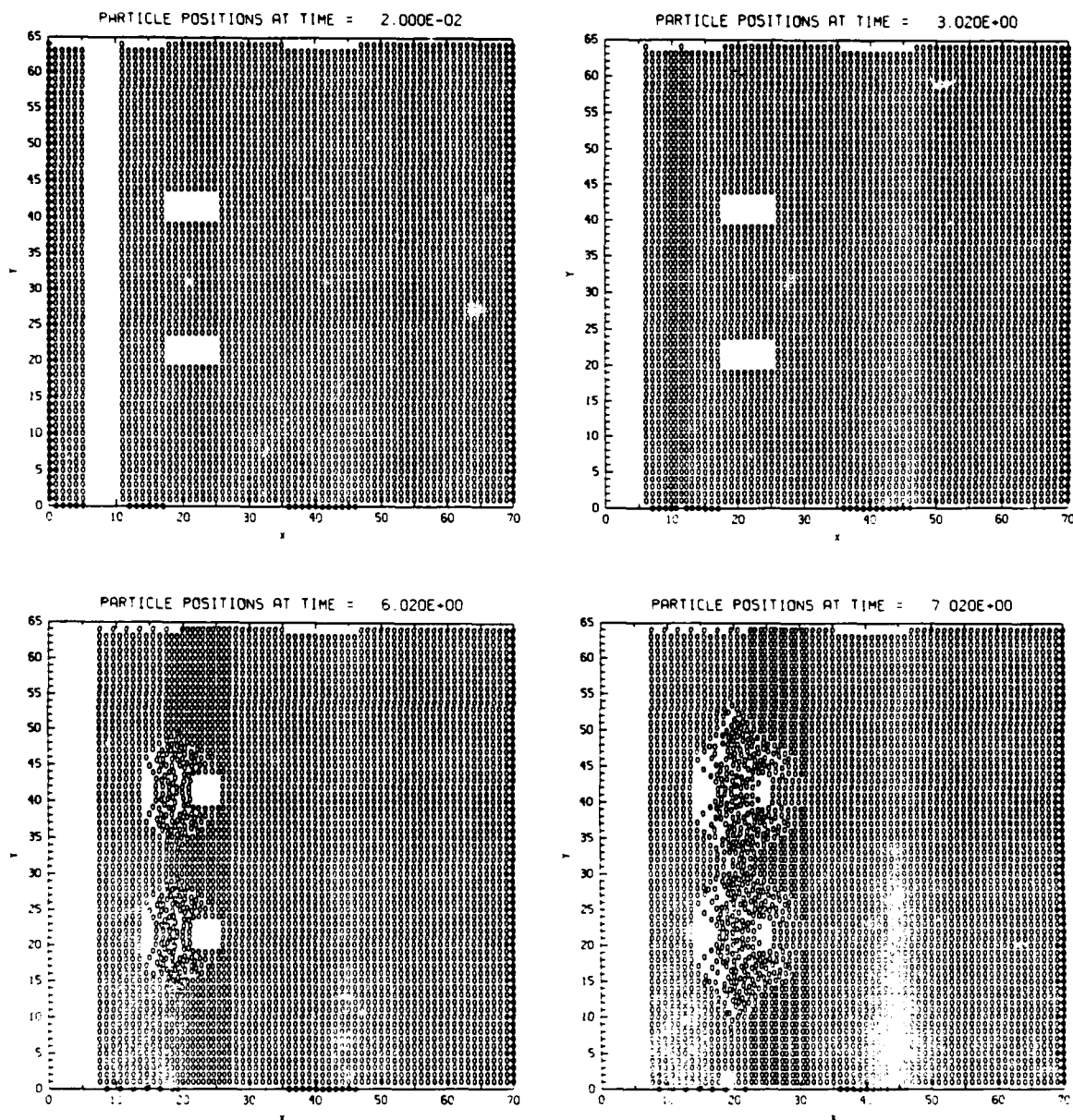


Figure 2: Particle positions for 4k particles in two dimensions. A "flying plate" impinges from the left, and has just made contact at $t = 3$; the resulting shock interacts with two rectangular voids.

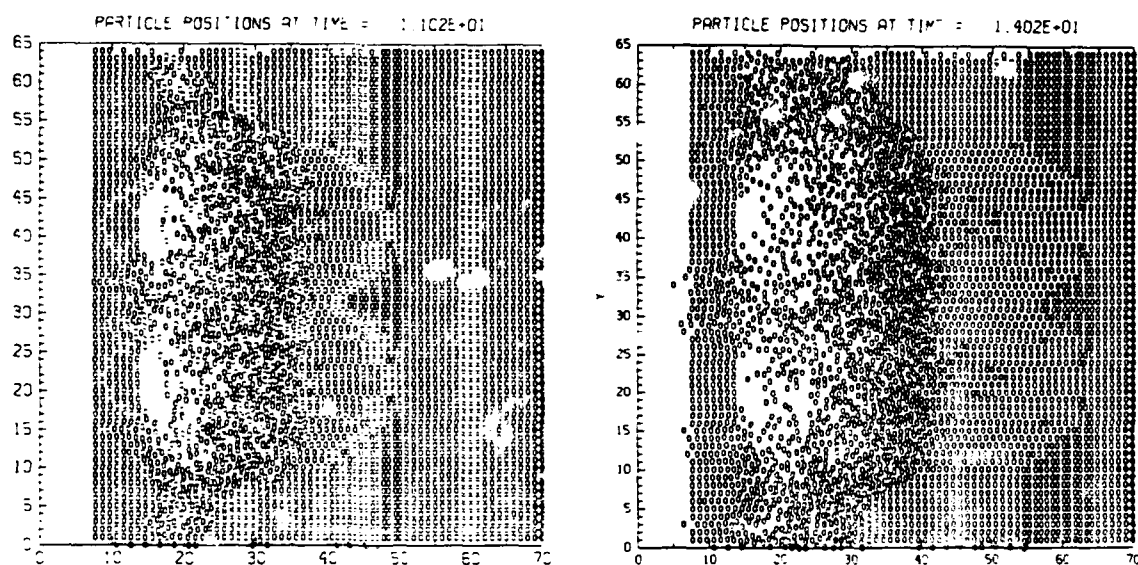


Figure 2: Particle positions for 4k particles in two dimensions. A “flying plate” impinges from the left, and has just made contact at $t = 3$; the resulting shock interacts with two rectangular voids.

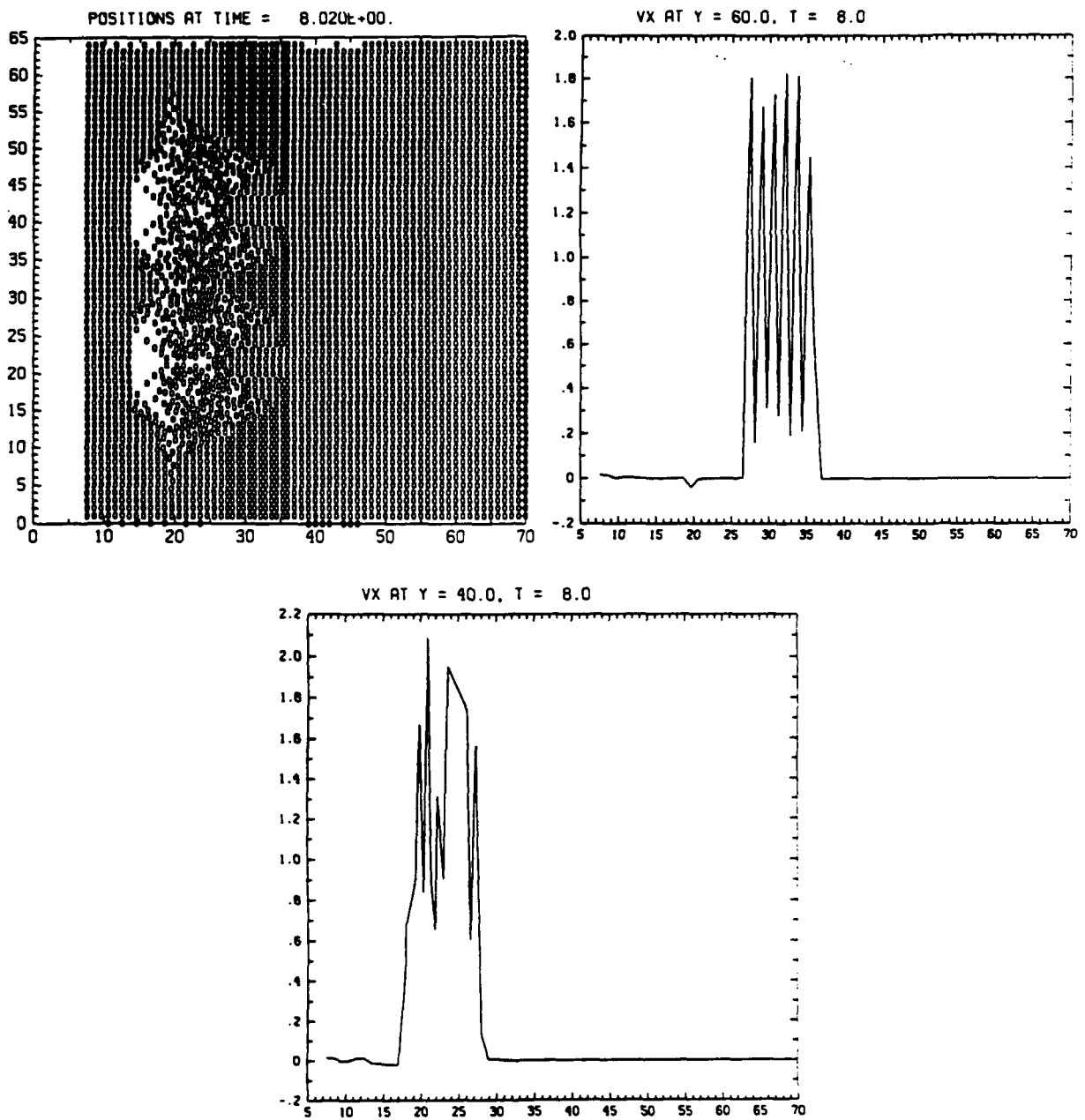


Figure 3: Profiles of x -directed velocity at two indicated y positions for the same calculation illustrated in figure 2.

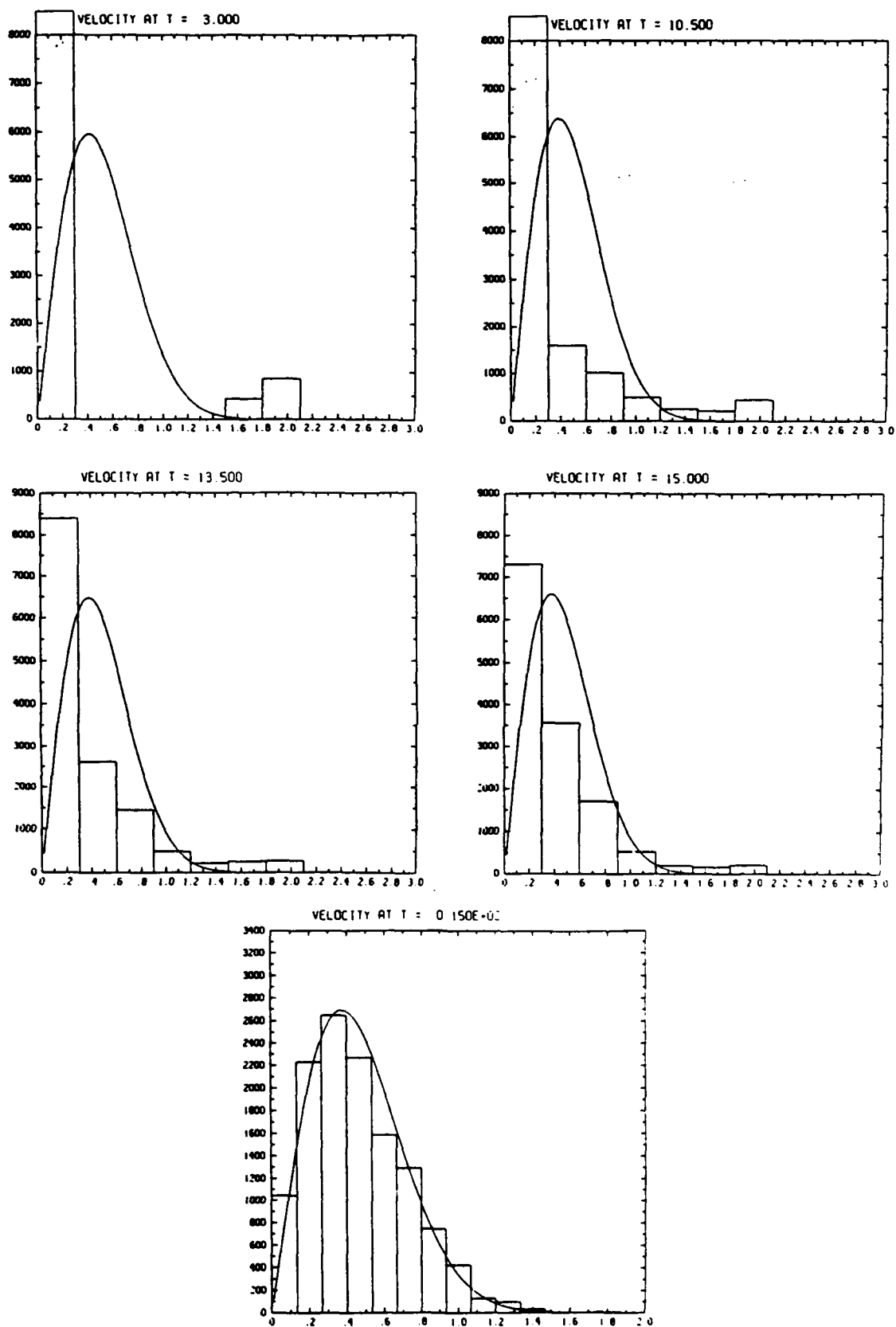


Figure 4: Velocity distribution histograms with superimposed equilibrium distributions, for the same calculation illustrated in figure 2.

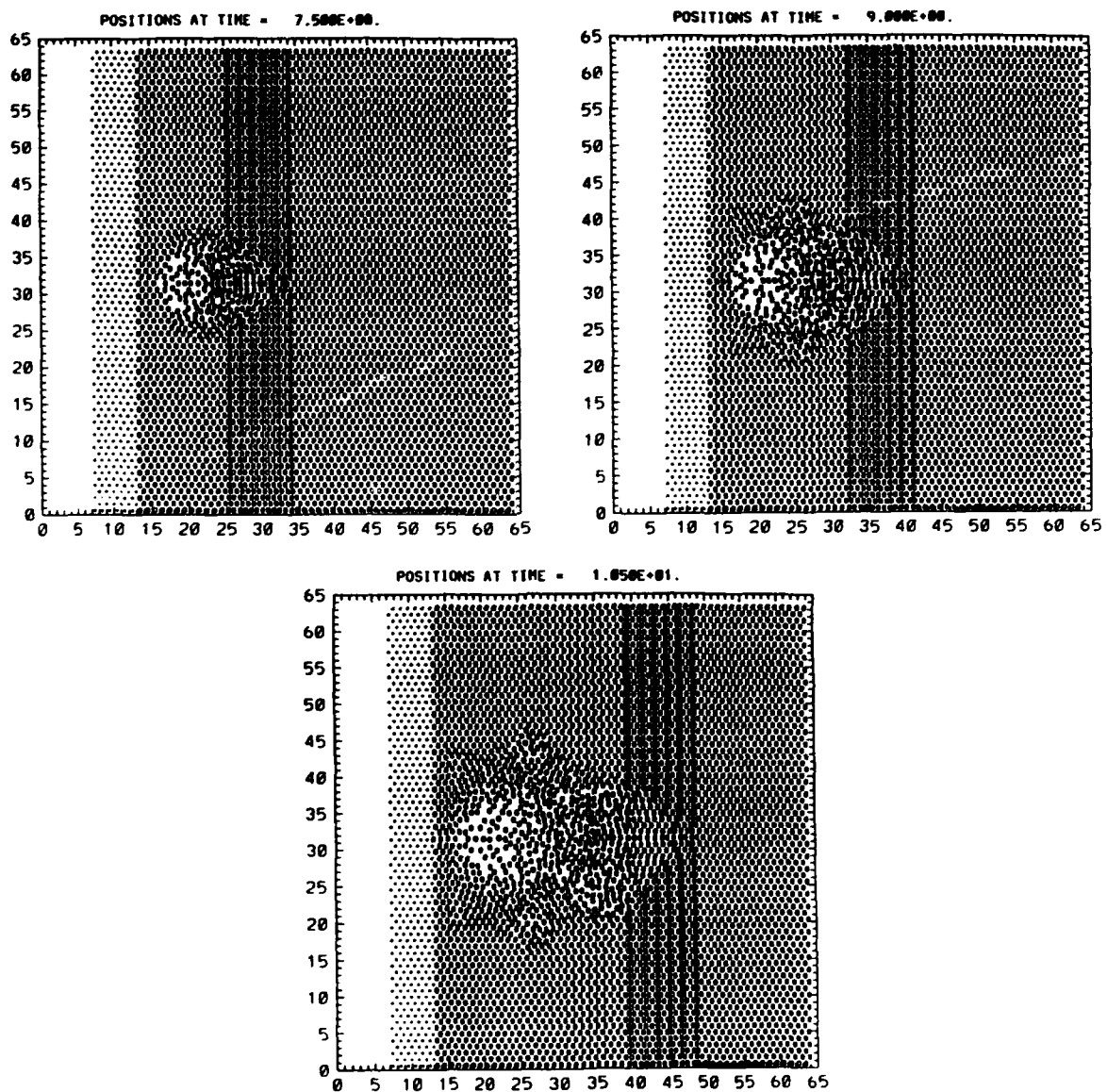


Figure 5: A void in a hexagonal lattice interacting with a shock launched by a flying plate.

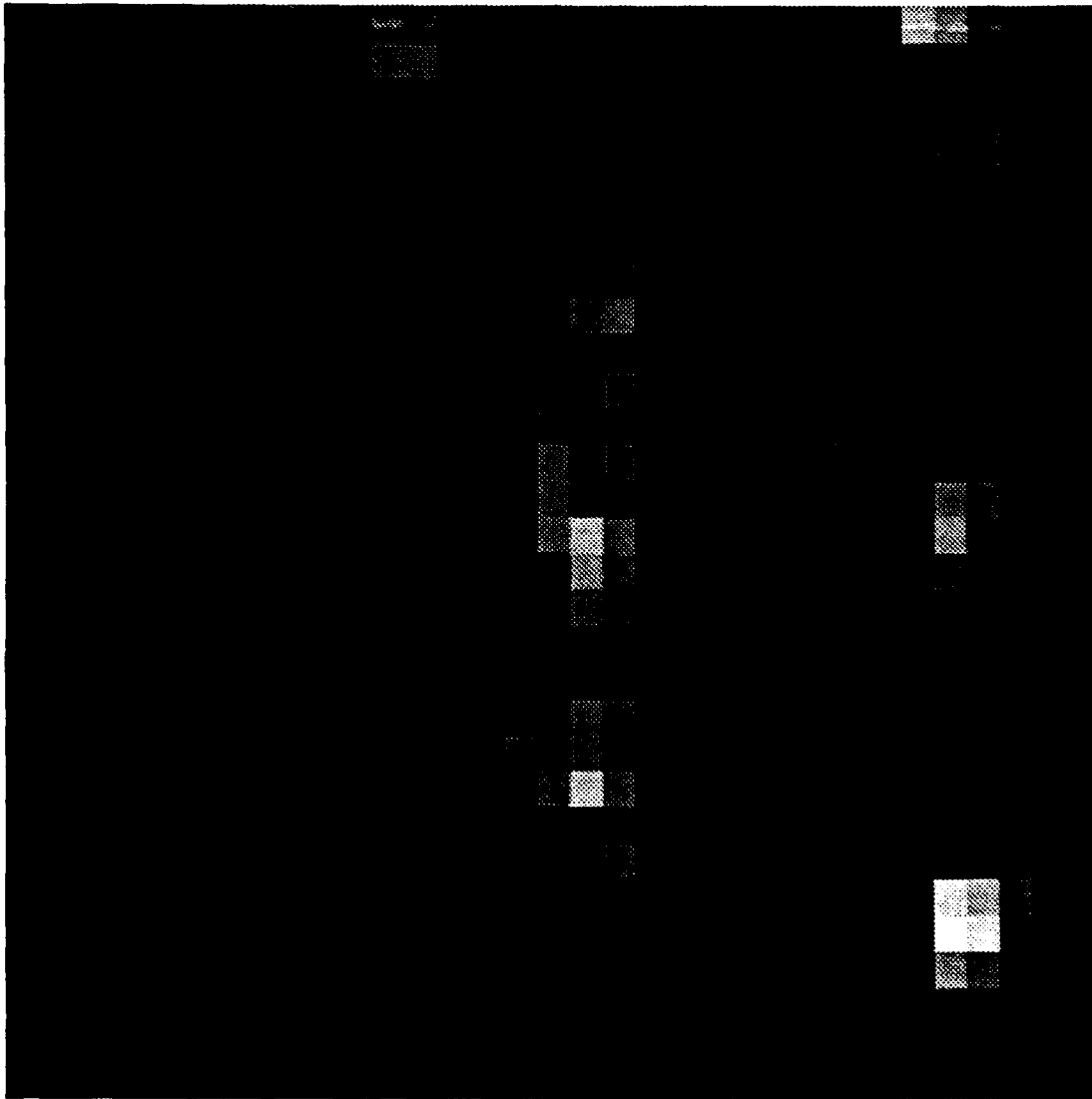


Figure 6: Scaled, smoothed density plot corresponding to the same calculation illustrated in figure 2, at $t = 13.5$. Increasing brightness indicates increasing density. The three bright patches near the right hand side of the figure correspond to the compression at the location of the void-interrupted shock.

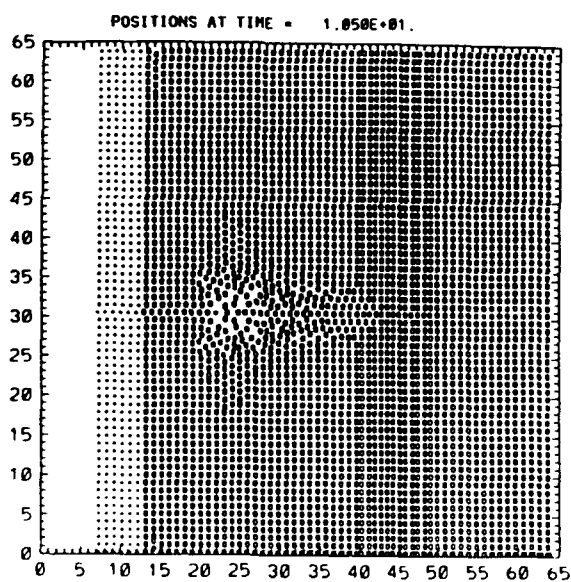
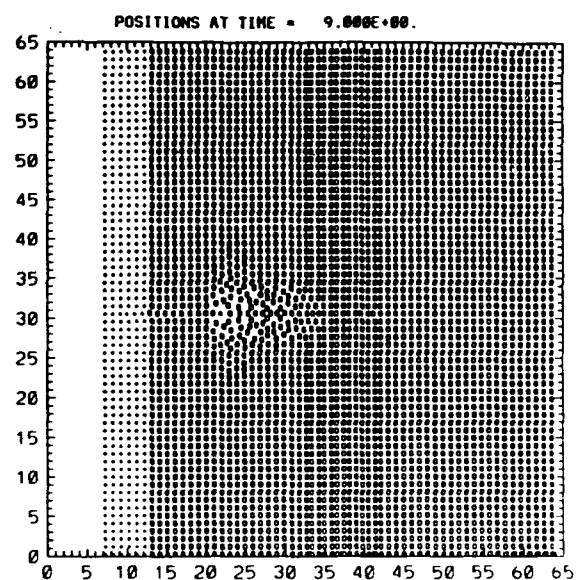
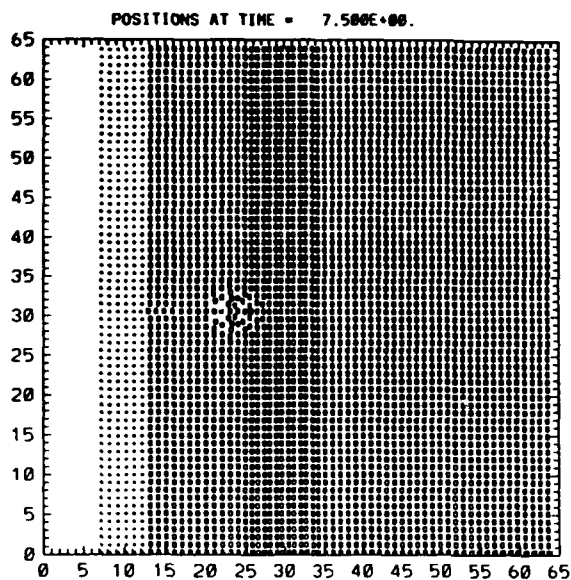


Figure 7: A mass defect in a square lattice interacting with a shock launched by a flying plate. The black square is a molecule with a mass excess of %50.

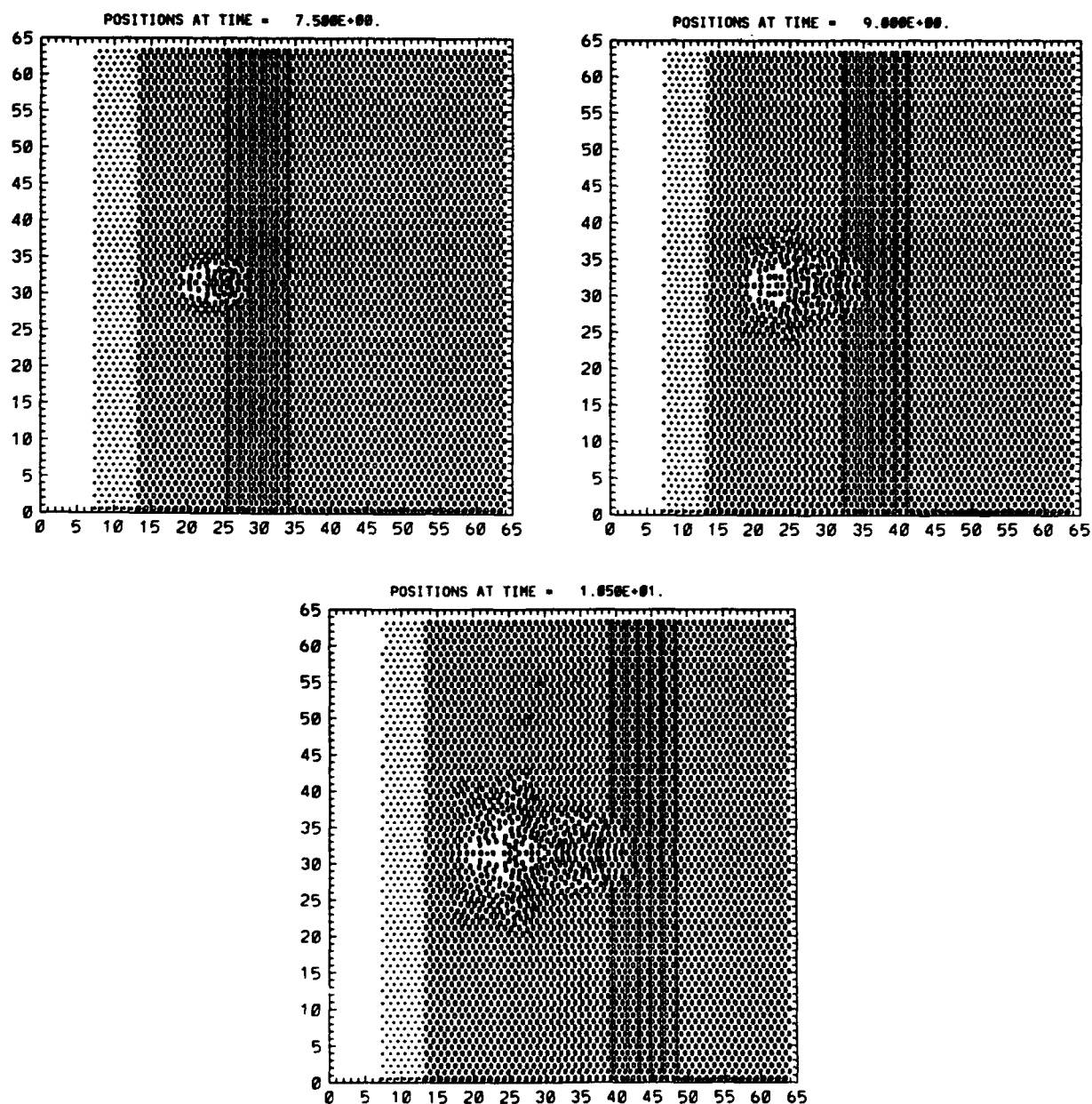


Figure 8: A mass defect in a hexagonal lattice interacting with a shock launched by a flying plate. The black square is a molecule with a mass excess of %50.

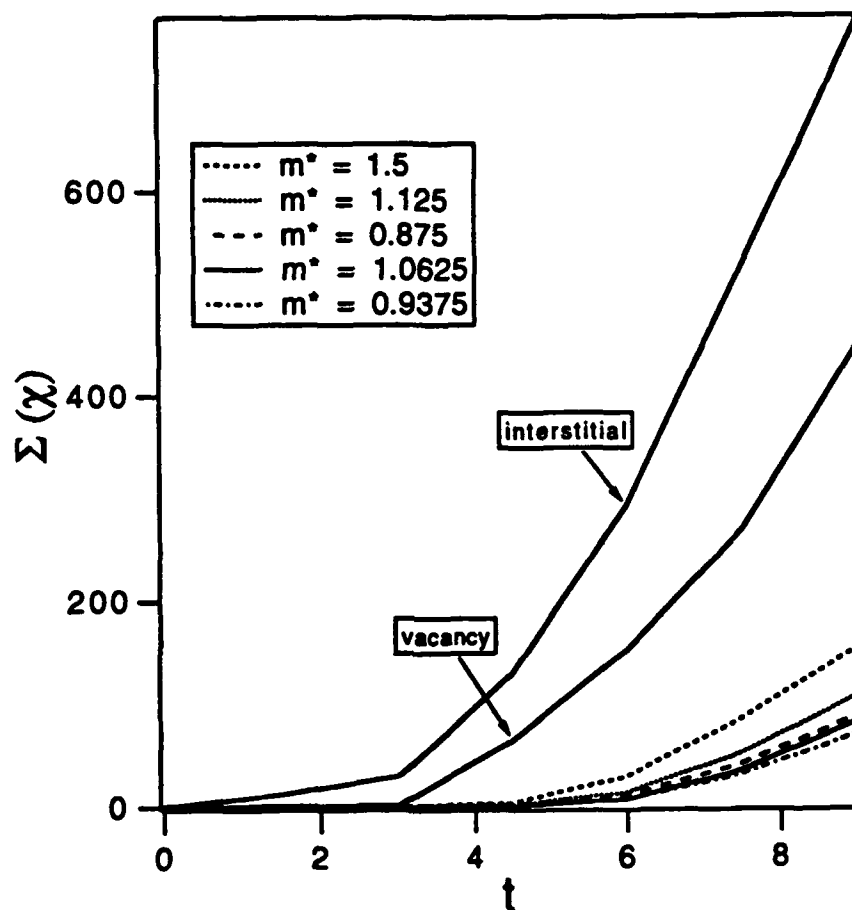


Figure 9: The disruption factor as a function of time, for several types of defects in a square lattice.

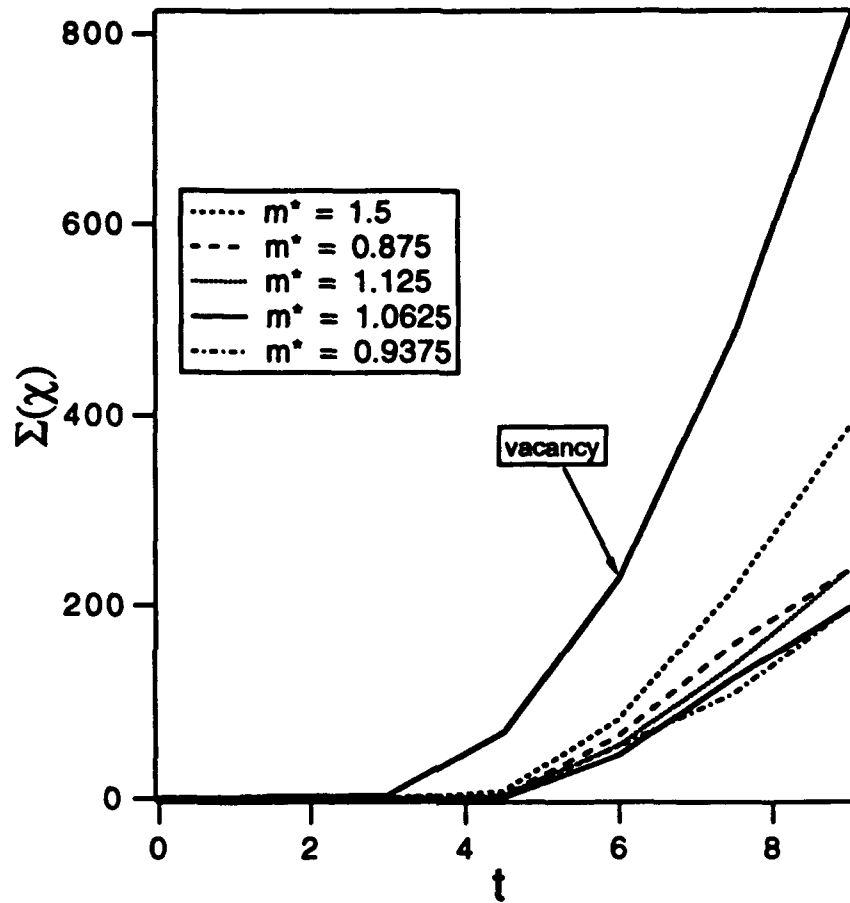


Figure 10: The disruption factor as a function of time, for mass defects of several values and for a vacancy in a hexagonal lattice.

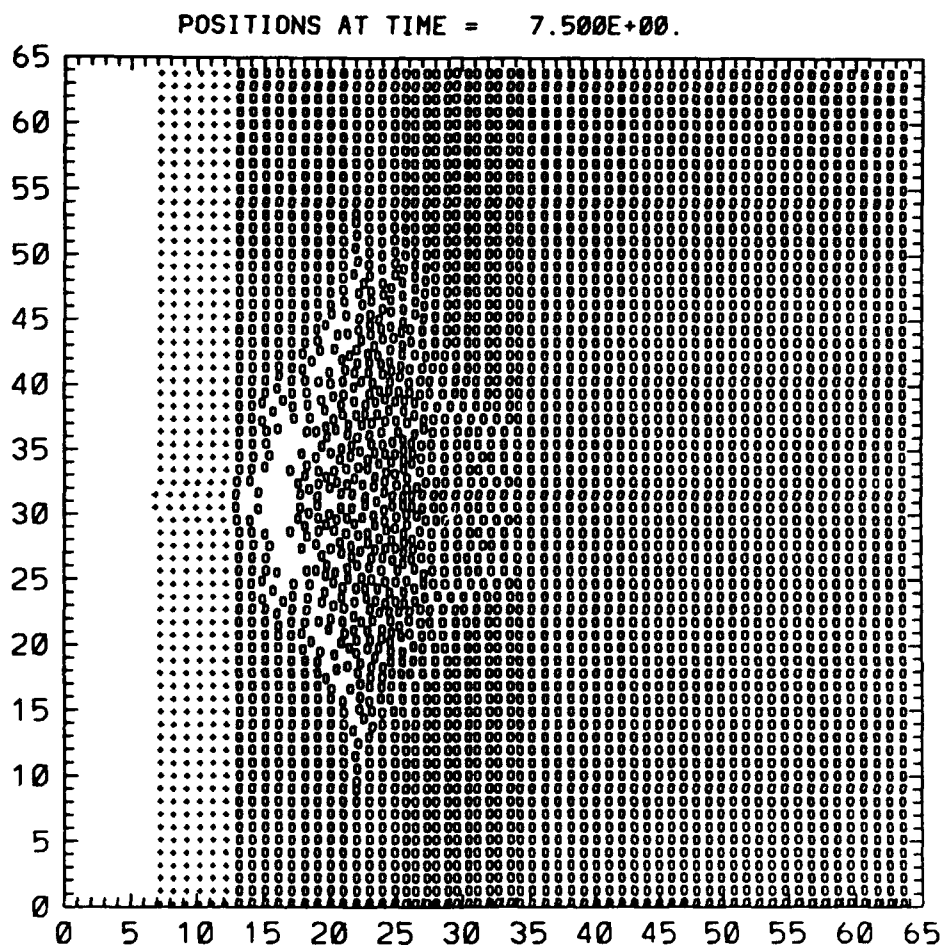


Figure 11: An interstitial inclusion in a square lattice.

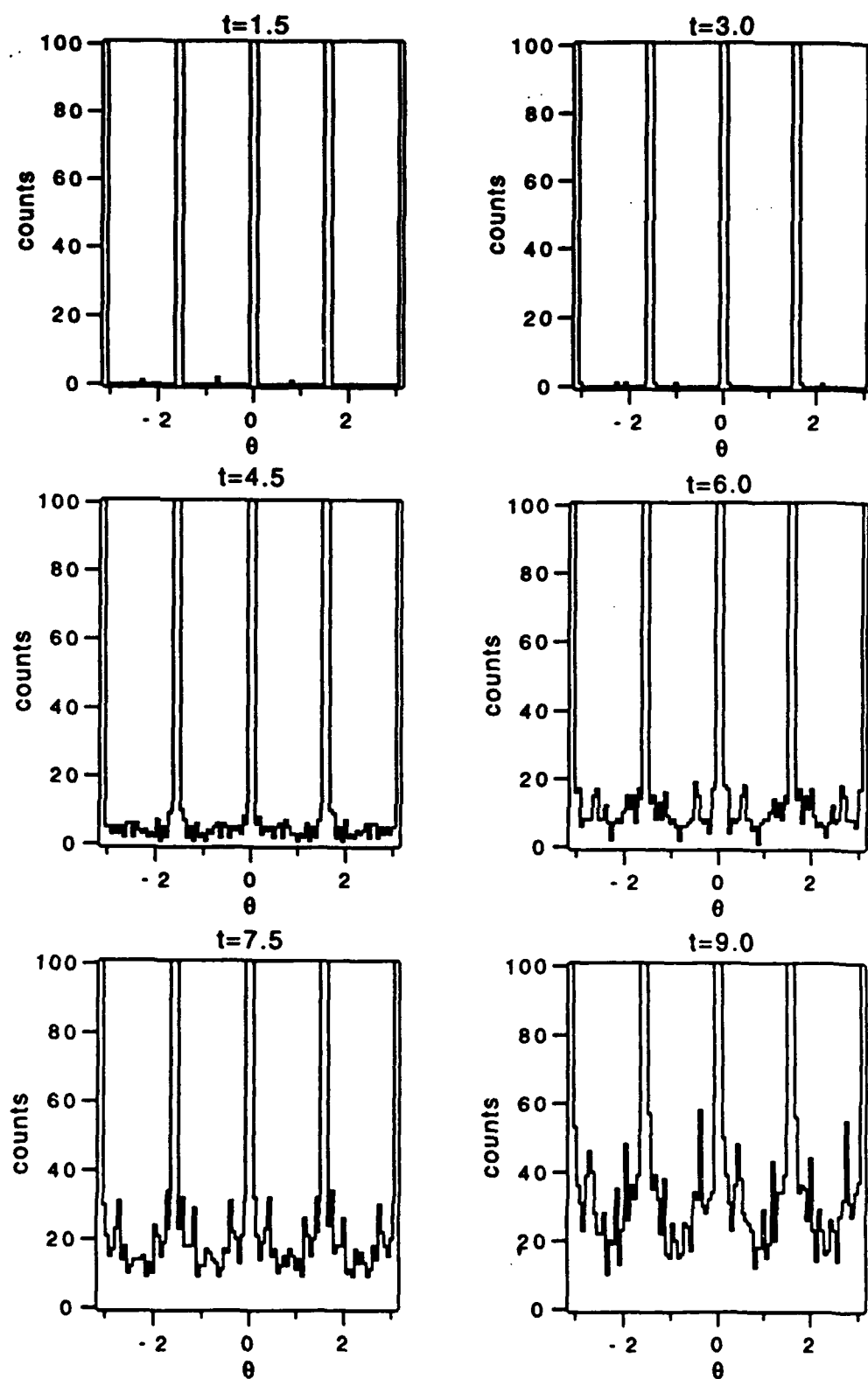


Figure 12: The evolution of the distribution of intermolecular bond angles in a square lattice as the shock front passes through a lattice vacancy.

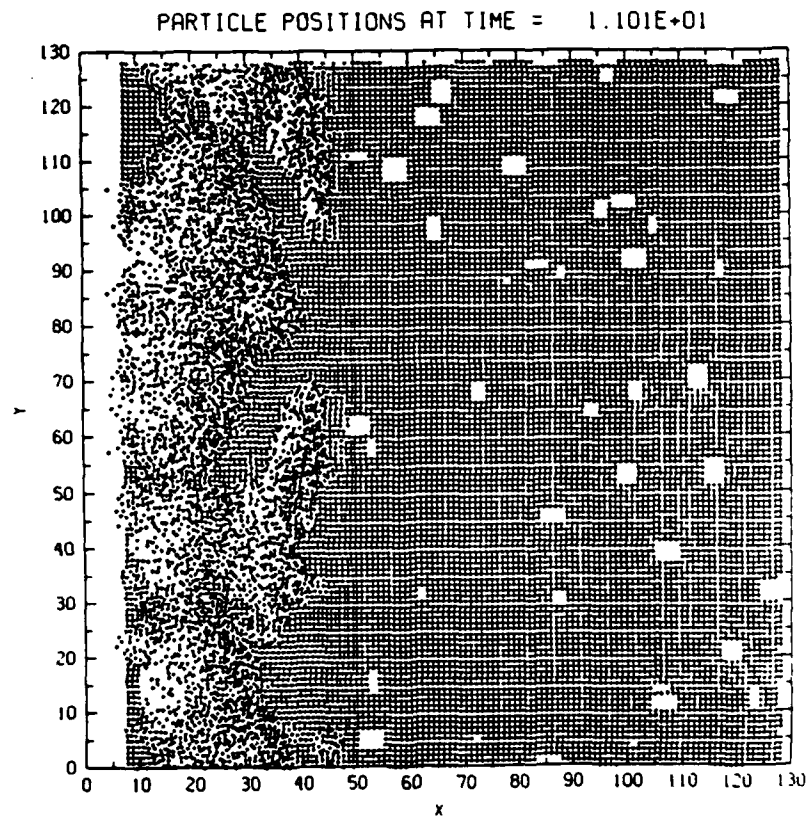
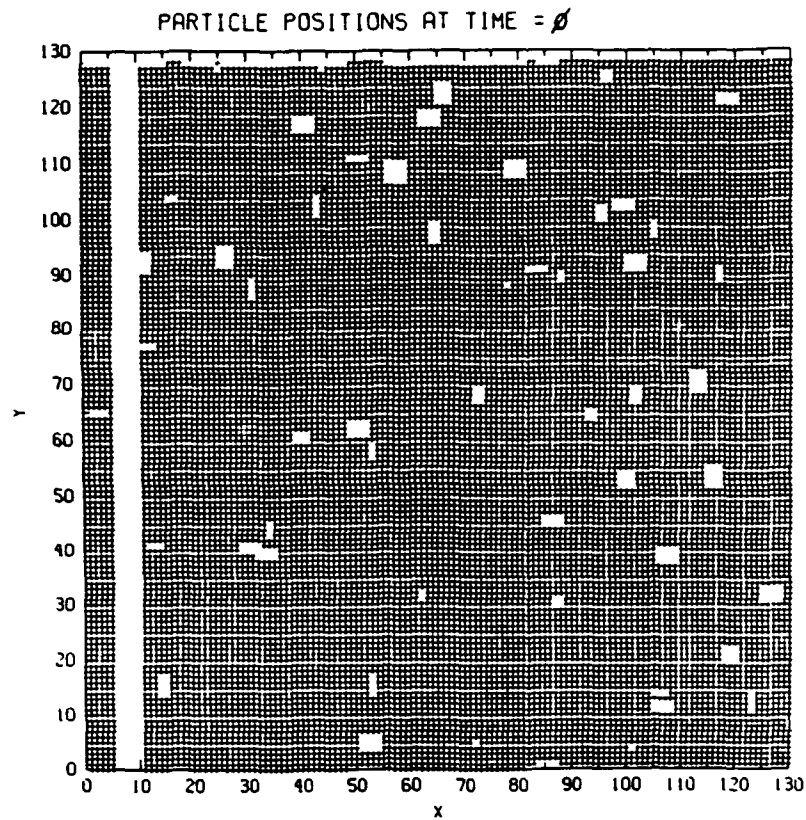


Figure 13: Particle positions in a 32k particle system, with a random distribution of voids. Again a flying plate has launched a shock from the left. Only the left half (approximately 16k particles) of the total system is shown.

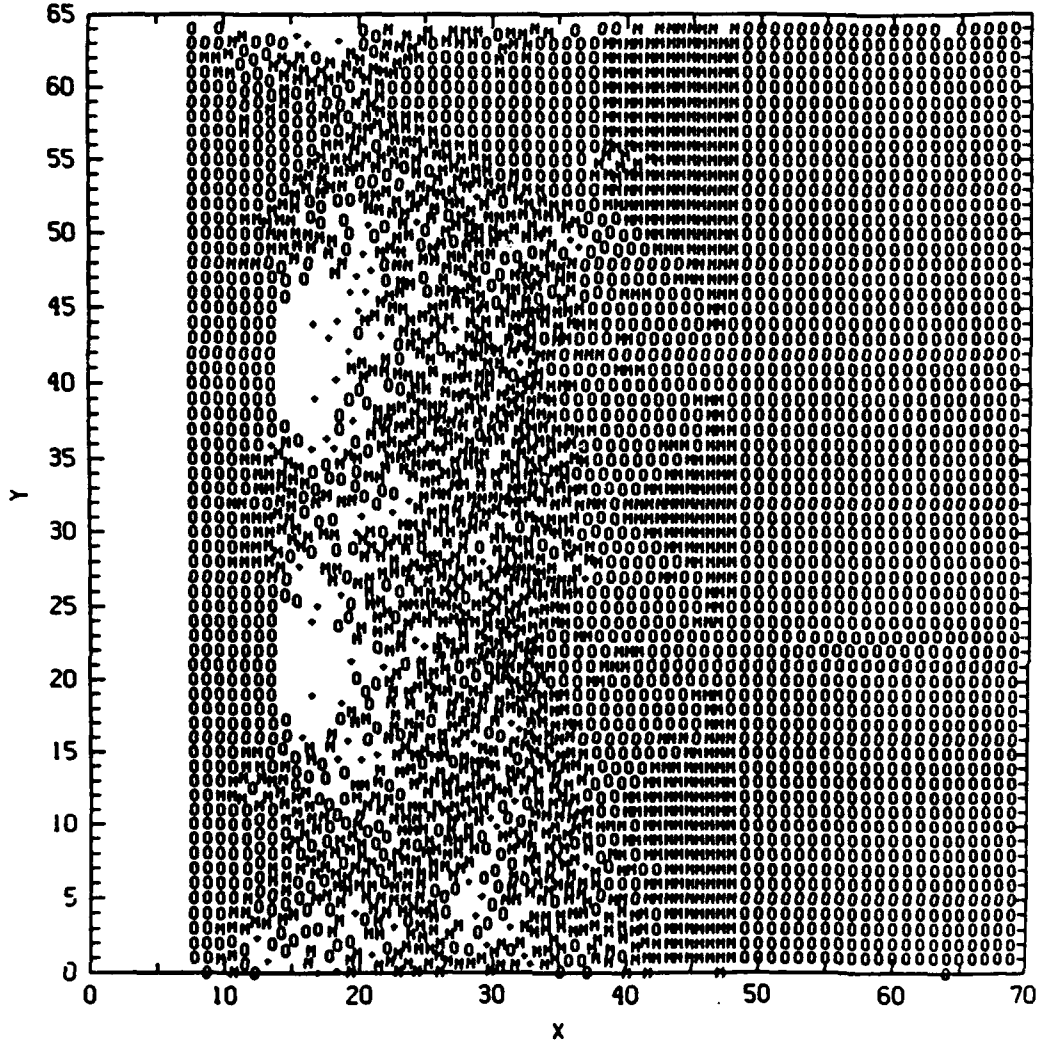


Figure 14: The quantity $\nabla \cdot F$ for calculation illustrated in figure 2, at $t = 10.5$. "+" symbols indicate the positions of particles with a $\nabla \cdot F > 0$, and "M" indicates the positions of particles with a $\nabla \cdot F < 0$.

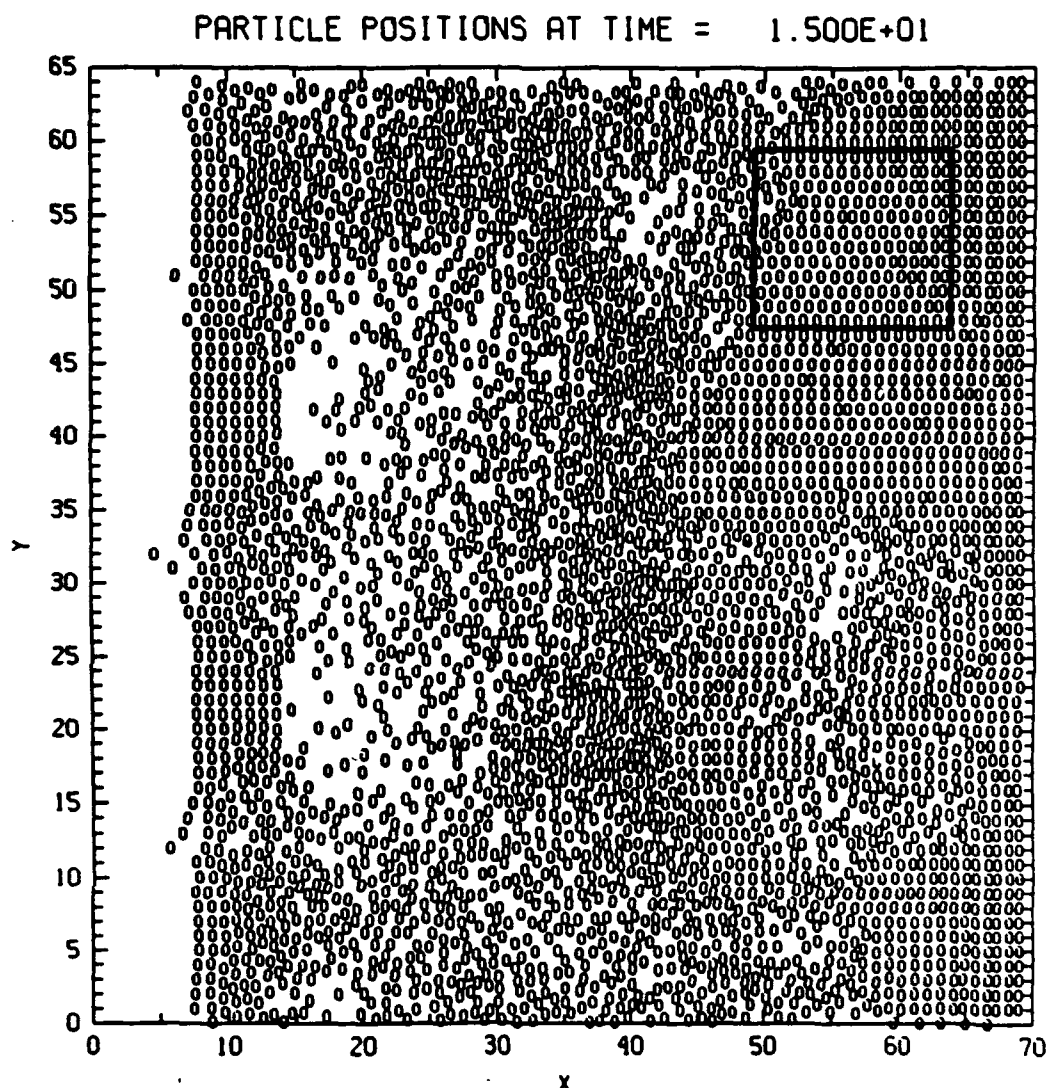


Figure 15: A frame from a later time, $t = 15$, in the calculation illustrated in figure 2, showing the emergence of an hexagonal phase embedded in the predominant square-symmetric crystal. A box has been drawn around the hexagonal region.

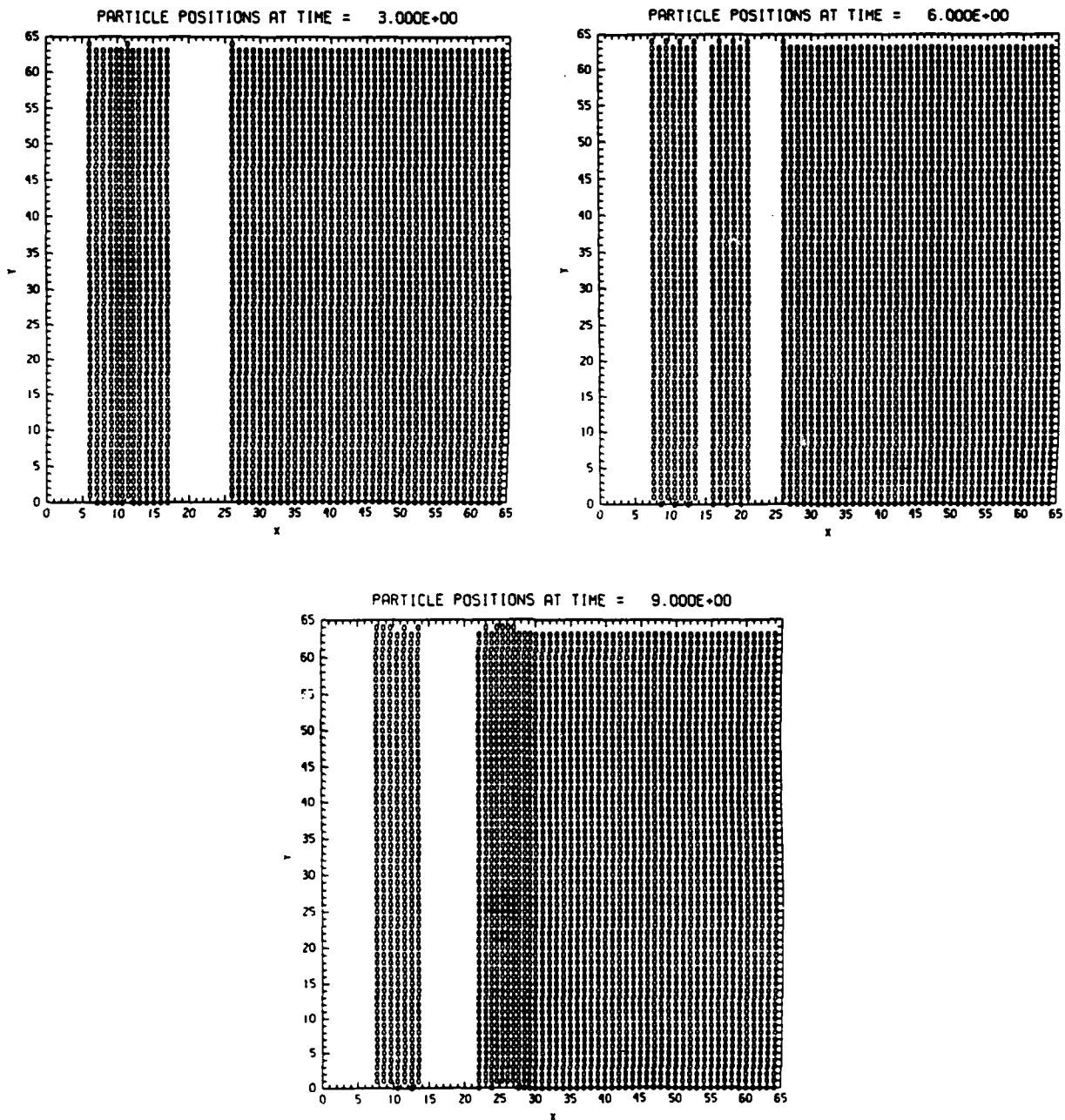


Figure 16: A sequence of particle position plots similar to those in figure 2, but with the two voids replaced by a continuous gap.

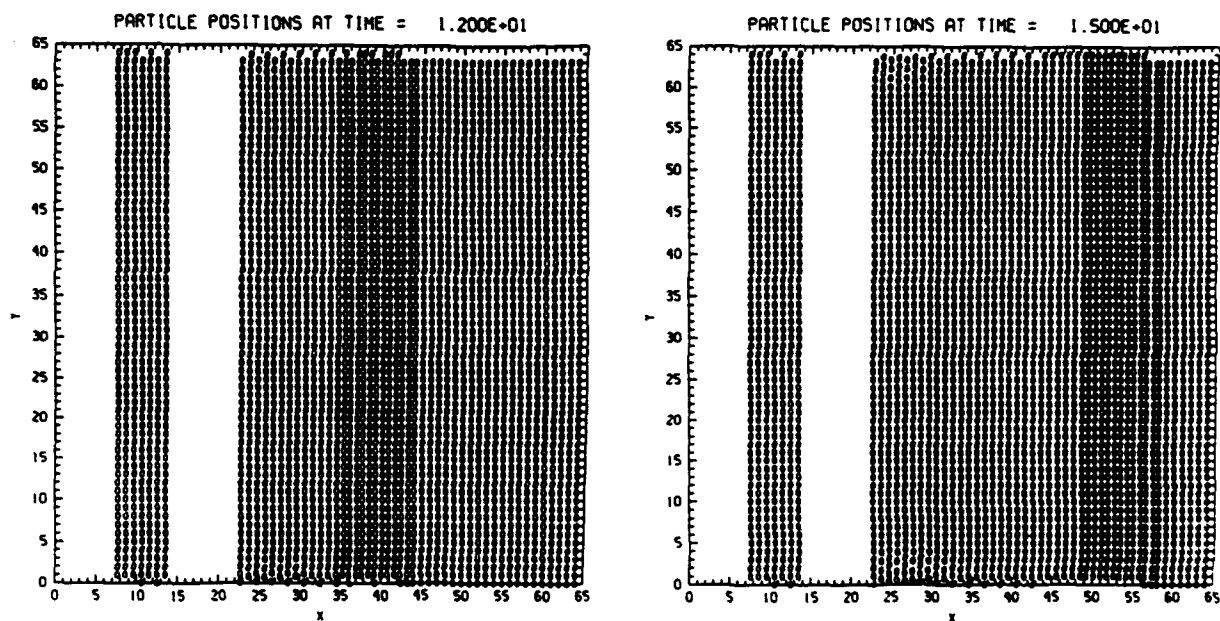


Figure 16: A sequence of particle position plots similar to those in figure 2, but with the two voids replaced by a continuous gap.

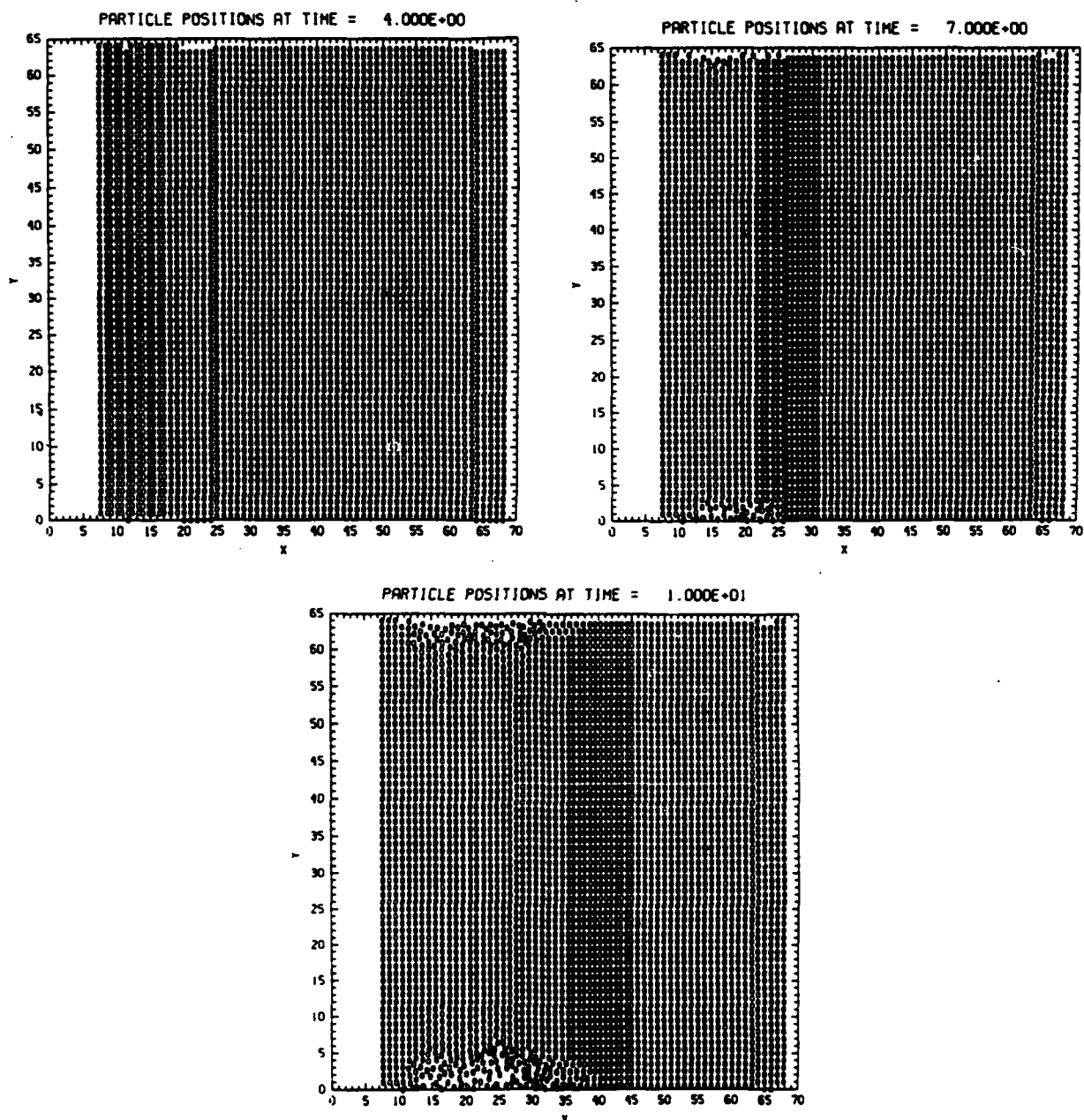


Figure 17: Particle position plot of a shock progressing through a linear defect and two small voids at $x = 24.5$